Aggregation of liposomes in presence of La^{3+}: A study of the fractal dimension

Juan Sabín, Gerardo Prieto, Juan M. Ruso, Paula Messina,* and Félix Sarmiento†

Biophysics and Interfaces Group, Department of Applied Physics, Faculty of Physics, University of Santiago de Compostela, E-15782 Santiago de Compostela, Spain

(Received 8 March 2007; published 30 July 2007)

A study of the fractal dimension of the aggregation of three different types of large unilamellar vesicles, formed by egg yolk phosphatidylcholine (EYPC), dimyristoyl-phosphocholine (DMPC), and dipalmitoyl-phosphocholine (DPPC), in the presence of La^{3+}, is presented. Aggregate liposome fractal dimensions were calculated by two methods, aggregation kinetics, using the approaches diffusion-limited cluster aggregation (DLCA) and reaction-limited cluster aggregation (RLCA) and angle-scattering light dispersion. Electrophoretic measurements show a similar variation of the zeta potential (ζ potential) for EYPC and DPPC, with a small increase of initial positive values. However, the ζ potential of DMPC changes from a initial negative value to near zero with increasing La^{3+} concentration. The evolution of the aggregate sizes was followed by light scattering. DPPC and DMPC show a RLCA regimen growth at low La^{3+} concentrations and a DLCA regimen at higher concentrations. In the case of EYPC, the final size of aggregation strongly depends on La^{3+} concentration. The calculated fractal dimension is in the range 1.8 to 2.1.

DOI: 10.1103/PhysRevE.76.011408 PACS number(s): 61.43.Hv, 05.45.Df, 89.75.Fb, 87.68.+z

I. INTRODUCTION

Liposomes are spherical, self-closed structures composed of curved lipid bilayers which entrap part of the solvent into their interior [1]. They may consist of one or several concentric bilayers and their size ranges from 20 nm to several micrometers [2]. Liposomes have been the subject of extensive experimental study due to their importance as a drug delivery system and to their value as a model system for more complex biological membranes [3]. An important phenomenon, from both a theoretical and applied perspective, is the membrane-membrane interaction between bilayer membranes. The large structures that liposomes form when they aggregate produce good models for further analysis. These structures are disorderly in nature but can be quite well described in terms of fractal geometry [4]. The fractal geometry of colloidal particle aggregates play an important role in their physical behavior.

The fractal dimension characterizes how the monomers occupy space in the aggregates [5]. The first experiments that explicitly investigated the fractal nature of aggregates were reported in 1979 by Forrest and Witten. In these experiments, metallic oxide smoke particles were deposited onto transmission electron microscopy (TEM) substrates and their fractal dimensions determined using image analysis techniques [6]. Nowadays, there are numerous fractal studies characterizing the aggregation of silica [7,8], proteins [9–11], gold [12], or polystyrene latex [5,13,14].

From a theoretical point of view, the introduction of the diffusion-limited aggregation model (DLA) by Witten and Sander [15] in 1981 has improved studies of fractal geometry in colloidal aggregation. In this model, particles are added one at a time to a growing cluster or aggregate of particles, via random walk trajectories, starting from outside of the region occupied by the cluster. The structures generated in this way are random ramified clusters with a determined fractal dimension [16]. An extension of this model, the diffusion-limited cluster aggregation (DLCA) [17–19], considers that the clusters can interact with each other to form clusters of greater size. In this model the sticking probability is equal to one and all the collisions between particles are effective.

Another model is the reaction-limited cluster aggregation (RLCA) [20], for which a large number of collisions are needed before the particles bind. Obviously, in this case the sticking probability is smaller than one. Studies of the aggregates by application of these models have been made in some detail by simulations and experiments on small-angle neutron scattering [21,22] or by Monte Carlo simulations [23,24].

The results have shown that DLCA clusters have a fractal dimension of $d_f \approx 2.1$ and the kinetics of aggregation are characterized by a power-law growth for the average radius of gyration,

$$R_g \propto t^{1/d_f}, \tag{1}$$

while RLCA clusters have a fractal dimension of $d_f \approx 1.8$ and the growth is exponential,

$$R_g \propto e^{\alpha t}. \tag{2}$$

Light scattering has been extensively used in the study of the fractal dimension aggregation. In static light scattering, a beam of light is directed onto a sample and the scattered intensity is measured as a function of the magnitude of the scattering vector, q, with

$$q = \frac{4\pi n_0 \sin(\theta/2)}{\lambda_0}, \tag{3}$$

where n_0 is the refractive index of the dispersion medium, θ is the scattering angle, and λ_0 is the wavelength of the incident light. If the individual particles in a fractal aggregate are

*Present address: Department of Chemistry, National University of Sud, Bahía Blanca, Argentina.

†Author to whom correspondence should be addressed. Fax: +34 981 520 676; fsarmi@usc.es

monodisperse, the scattered intensity $I(Q)$ by an aggregate can be written as

$$I(q) \propto P(q)S(q). \tag{4}$$

In the above expression, $P(q)$ is related to the shape of the single particle and $S(q)$ is the interparticle structure factor, which represents the correlations between different primary particles within an aggregate, assuming that there are no correlations between the aggregates themselves. Thus, it describes the spatial arrangement of the particles in an aggregate [4]. At large values of q, $S(q)$ is approximately equal to 1. The scattered intensity is then dominated by the single particle form factor and only the scattering due to individual particles is seen. At small q values compared to $1/r_0$, but large compared to $1/R_G$, r_0 being the radius of the monomer and R_G being the radius of the aggregate (i.e., $1/R_G \ll q \ll 1/r_0$), $P(Q) \approx 1$ and $S(Q)$ reduces to [25]

$$S(q) \propto q^{-d_f}. \tag{5}$$

Hence, provided that R_G is much larger than r_0, Eq. (4) takes the form of the well-known scattering power law,

$$I(q) \propto S(q) \propto q^{-d_f}. \tag{6}$$

In accordance to the previous information, we can calculate the fractal dimension of the aggregates of liposomes by two methods using light scattering.

In previous works we studied the colloidal stability of the liposomes in the presence of different ions under the Derjaguin-Landau-Verwey-Overbeek (DLVO) theory [26,27] focusing on the range of concentrations of ions in which the liposomes are stable [28,29]. We found that liposomes are unstable at trivalent ion concentrations above 0.1–0.2 M due to aggregation processes [28,30]. The goal of this work is to characterize the aggregation of liposomes composed of different cholines [egg yolk phosphatidylcholine (EYPC), dipalmitoyl-phosphocholine (DPPC), and dimyristoyl-phosphocholine (DMPC)] and to determine their fractal dimension. The aggregation of the liposomes has been induced by the addition of La^{3+} at different concentrations. The fractal dimension was calculated by two methods: first, following the evolution of the size of the aggregates during the process and second, measuring the scattering light dispersion of the final aggregates.

II. EXPERIMENTAL METHOD

A. Materials

L-α-phosphatidylcholine from egg yolk (EYPC) (No. P 3556), 1,2-dimyristoyl-sn-glycero-3-phosphocholine (DMPC) (No. P 2663), 1,2-dipalmitoyl-sn-glycero-3-phosphocholine (DPPC) (No. P 0763) with 99% purity were purchased from Sigma and used as received. Lanthanum nitrate hexahydrate with a purity of 99.999% was purchased from Aldrich (No. 203548). Organic solvents, methanol and chloroform, were supplied by Aldrich and Merck, respectively. Polycarbonate membranes were purchased from Millipore.

B. Vesicle preparation

Large unilamellar vesicles (LUVs) were prepared by the thin-film hydration method [13]. A solution of phospholipid in chloroform and methanol was dried in a rotary evaporator under a stream of nitrogen. The resultant lipid film was hydrated with double distilled, degassed, and deionized water. This mixture was extruded five times through polycarbonate filters of 800 nm pore size and five times through polycarbonate filters of 200 nm to form LUVs.

C. Transmission electron microscopy

The morphological examination of the liposomes was performed by transmission electron microscopy (TEM) (CM-12 Philips). The samples were stained with 2% (w/v) phosphotungstic acid and placed on copper grids with Formvart films for viewing by TEM.

D. Electrophorectic measurements

Electrophorectic measurements of the liposome systems were measured using a Malvern Instruments Zetamaster 5002 by taking the average of five measurements. The cell used was a 5 mm$\times$2 mm rectangular quartz capillary. The temperature of the experiments was 298.15$\pm$0.01 K and was controlled by a Haake temperature controller. The zeta potentials (ζ potentials) were calculated from the electrophoretic motilities, μ_E, by means of the Henry correction of the Smoluchowski equation [31],

$$\zeta = \frac{3\mu_E \eta}{2\varepsilon_0 \varepsilon_r} \frac{1}{f(\kappa a)}, \tag{7}$$

where ε_0 is the permittivity of the vacuum, ε_r is the relative permittivity, a is the particle radius, κ is the Debye length, and η is the viscosity of water. The function $f(\kappa a)$ depends on the particle shape and for our system was determined by

$$f(\kappa a) = \frac{3}{2} - \frac{9}{2\kappa a} + \frac{75}{2\kappa^2 a^2}, \tag{8}$$

which is valid for $\kappa a > 1$.

E. Light scattering

Static and dynamic light scattering measurements were made at 298.15$\pm$0.01 K and an angle of 90° using a Spectrometer Autosizer 4800 from Malvern Instruments equipped with a Uniphase 75 mW Ar laser operating at 488 nm with vertically polarized light. Time correlation was analyzed by a digital autocorrelator PCS7132 from Malvern Instruments and the correlation function obtained was analyzed by the CONTIN algorithm, which gives the distribution of intensities dispersed by the system. The evolution of the aggregations was followed by measuring the radius of a cluster every 15 seconds. Scattering light measurements were made after the aggregates reached a stationary condition. The range of scattering angle was $10° < \theta < 135°$ and the wave vector was $3\times10^{-6} < q < 3.2\times10^{-7}$ m^{-1}.

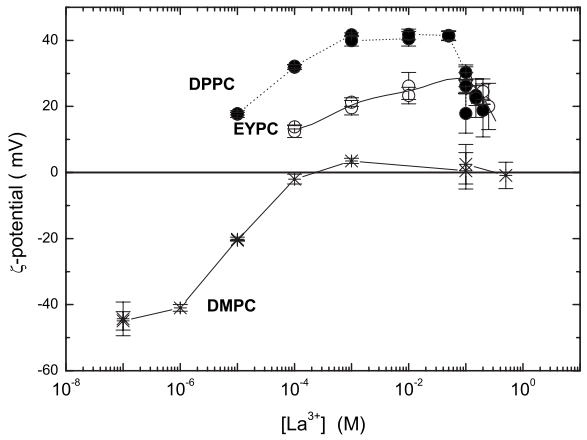

FIG. 1. Variation of ζ potential with the La^{3+} concentration for EYPC (○), DPPC (•), and DMPC (*) liposomes.

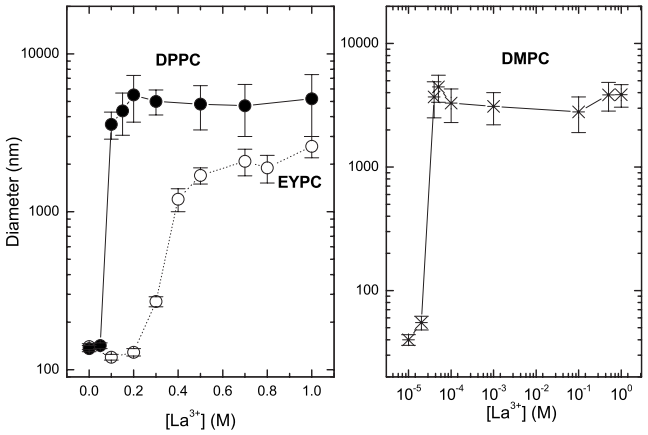

FIG. 2. Variation of the diameter of the aggregates with the La^{3+} concentration for EYPC (○), DPPC (•), and DMPC (*) liposomes.

III. RESULTS AND DISCUSSION

In this study, three different PC cholines were chosen, which have the same zwitterionic headgroup, but different tails. DMPC and DPPC are synthetic lipids with saturated double tails of 14 and 16 carbons, respectively. The EYPC cholines are natural lipids. They are mixtures of saturated and unsaturated lipids of different lengths [2]. Figure 1 shows the ζ potential for DPPC, DMPC, and EYPC liposomes at different concentrations of La^{3+}. DPPC and EYPC liposomes behave in similar ways. At low salt concentrations, they have a low positive ζ-potential value which increases due to the adsorption of La^{3+} ions, until a maximum is reached at around 0.1–0.2 M La^{3+}. For higher concentrations, the charge is screened due to the increase in the ionic strength of the medium and the ζ—potential values decrease for both types of liposomes. The DMPC liposomes have an initial negative ζ-potential value, which decreases (in absolute value) due to the strong adsorption of the positive La^{3+} ions to the negative surface of the DMPC liposomes. For concentrations above 10^{-4} M of La^{3+}, DMPC liposomes have a ζ-potential value near zero.

The ζ-potential values play an important role in the colloidal stability of liposomes. According to the classical DLVO theory, the stability of the particles in solution is predicted on the notion that two independent types of forces govern the interaction between similar colloidal particles immersed in polar solutions: attractive van der Waals forces and repulsive electrostatic forces. In liposomes with ζ potential near zero, the repulsive electrostatic barrier disappears and the interaction between liposomes is governed only by the attractive van der Waals forces, as observed in a RLCA or DLCA aggregation regimen.

Figure 2 shows the cluster sizes at different La^{3+} concentrations for each type of liposome measured when the stationary conditions have been reached. A drastic increase in the size of the liposomes indicates the threshold of the aggregation. Consistent with the classical DLVO theory, aggregation initiates when the ζ potential approaches zero as Figs. 1 and 2 show.

The evolution of the size of the aggregates was followed by light scattering at different La^{3+} concentrations for the three types of liposomes. The salt solutions were added 90 seconds after measuring was started. Figure 3 shows these results. DPPC liposomes exhibit the two typical types of aggregation behavior. For 0.1 and 0.12 M of La^{3+}, the growth in size follows the exponential [Eq. (2)], typical of the RLCA regimen. At higher concentrations, the DLCA regi-

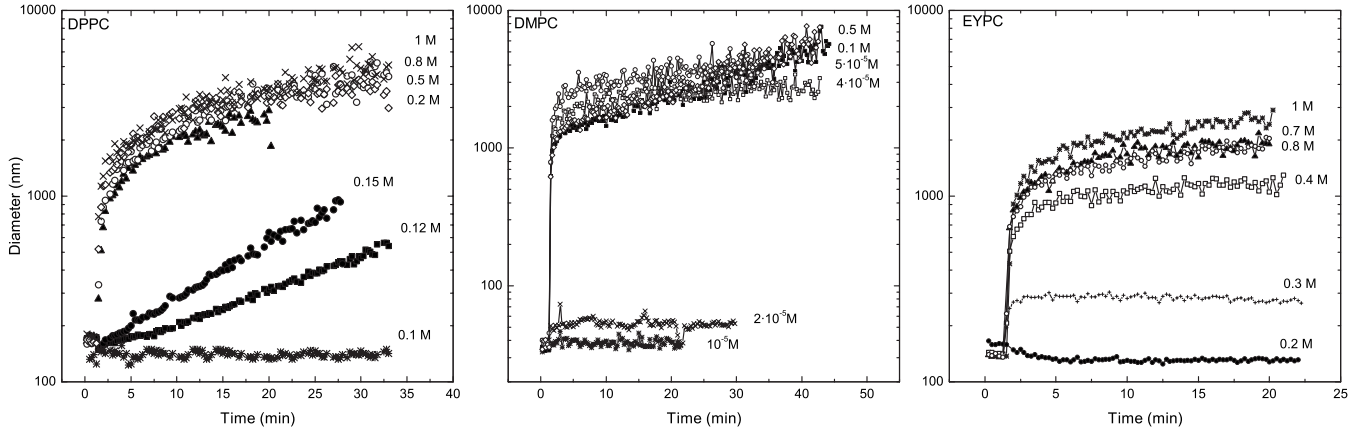

FIG. 3. Time evolution of the diameter of the aggregates for DPPC, DMPC, and EYPC liposomes.

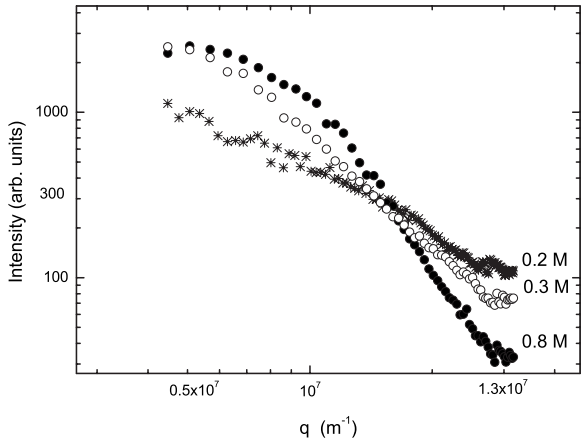

FIG. 4. Scattering intensity of EYPC liposomes in presence of 0.2 M (*), 0.3 M (◦), and 0.8 M (•) of La^{3+}.

men occurs and growth follows the power law of Eq. (1). Similar results were observed for DMPC liposomes although no RLCA regimen was observed. The EYPC results are of special interest because these liposomes behaved in unexpected ways: the final sizes of these aggregations seemed to depend on the concentration of La^{3+}. This unusual behavior is of great relevance because it allows the size of *stable aggregates* of EYPC liposomes to be controlled.

Once the liposomes were aggregated, the angular scattering light dispersed by the clusters was measured. Figure 4 shows the scattering intensity as a function of vector q for liposomes of EYPC in the presence of different La^{3+} concentrations. These measurements were also taken for DPPC and DMPC (data not shown).

Following Eqs. (1) and (6), the fractal dimension of the aggregates can be calculated from Figs. 3 and 4 by two different methods. Figures 5–7 show the fractal dimensions for DPPC, DMPC, and EYPC liposomes depending on the concentration of La^{3+}.

The values of the fractal dimensions are within the range predicted by computer simulations. The universal DLCA and

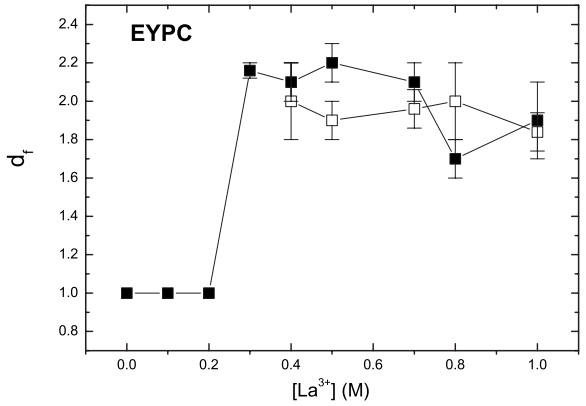

FIG. 6. Fractal dimension of the aggregates of EYPC liposomes at different concentration of La^{3+} calculated by scattering intensity measurements (■) and by time evolution of the diameters (□) of the clusters.

RLCA regimens were studied under ideal conditions and the interactions between clusters or between parts of clusters were not taken into account. Therefore, some variations from the computed simulated values were expected. However, there is a tendency to decrease from values near 2.1 (RLCA) to lower values near 1.8 (DLCA) as the La^{3+} concentration increases.

When the charge of the liposome is totally screened and the liposomes move similar to Brownian particles, there is a high probability that, as the particle moves from an exterior to an interior point of a cluster, it can intercept an arm of the cluster. Therefore, the growing arms will screen the interior of the cluster from incoming particles, resulting in an open structure with a low fractal dimension around 1.8 [32,33].

If the charge of the liposomes is not totally screened and there is some electrostatic repulsion between them, the sticking probability is less than 1 and the clusters will have to collide many times before they stick to each other [34]. This situation increases the possibility that the liposomes can reach an interior point of the clusters, resulting in compact

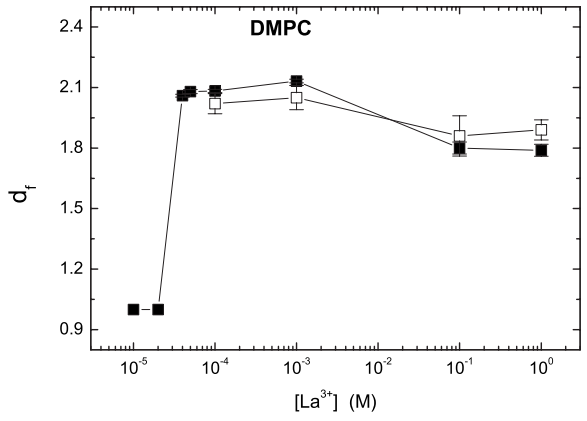

FIG. 5. Fractal dimension of the aggregates of DMPC liposomes at different concentrations of La^{3+} calculated by scattering intensity measurements (■) and by time evolution of the diameters (□) of the clusters.

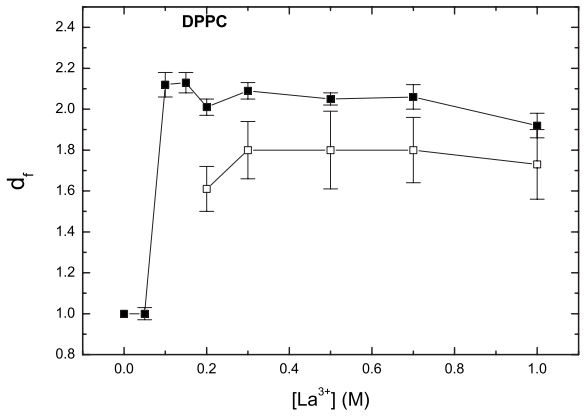

FIG. 7. Fractal dimension of the aggregates of DPPC liposomes at different concentration of La^{3+} calculated by scattering intensity measurements (■) and by time evolution of the diameters (□) of the clusters.

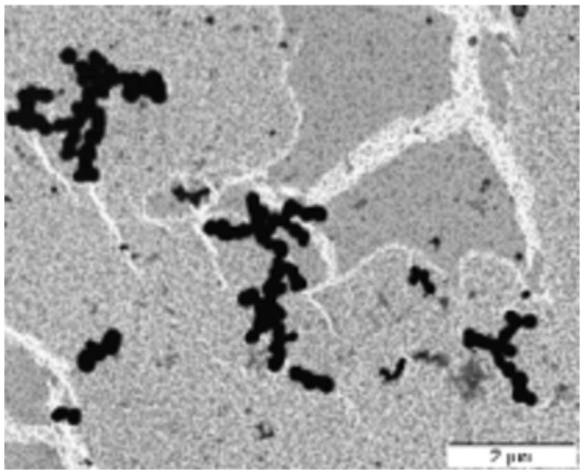

FIG. 8. TEM photograph of DPPC liposomes in the presence of 0.7 M of La^{3+}. DLCA clusters with open structures.

and spherical structures with a high fractal dimension around 2.1. Figures 8 and 9 are TEM micrographs of EYPC liposomes that illustrate the two different regimes of aggregation. Other authors have found similar results using optical microscopy [35] or atomic force microscopy [36].

We have focused on the characterization of the clusters of EYPC liposomes due to their unusual behavior in the aggregation process. It was confirmed that the aggregates are reversible by adding water to the solution. Figure 10 shows that the clusters return to their initial size when water is added if the final concentration of La^{3+} does not completely screen the charge of the liposomes. This effect only occurs with EYPC liposomes but not with DPPC or DMPC (inset Fig. 10). These results suggest that EYPC liposome aggregation occurs at a secondary minimum of the DLVO potential [37].

In a previous work [28] we found that when the electrostatic forces are totally screened, the total interaction potential between two liposomes consists of the sum of the van der Waals potential and the hydration potential. In this case the

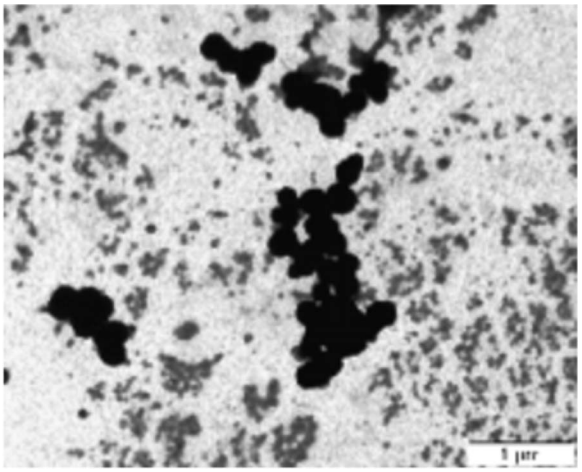

FIG. 9. TEM photograph of DPPC liposomes in the presence of 0.2 M of La^{3+}. RCLA clusters with closed and compact structures.

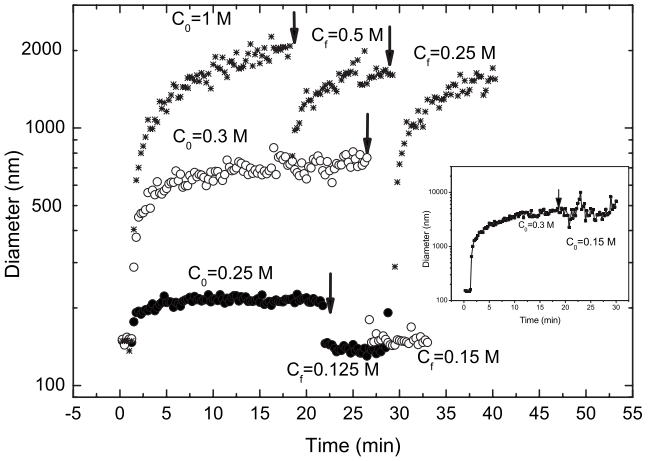

FIG. 10. Time evolution of the aggregates of EYPC liposomes at 0.25 M (•), 0.3 M (◦), and 1 M (*) of La^{3+}. The inset shows the time evolution of the aggregates of DPPC liposomes at 0.3 M. The arrows indicate the time when water was added to dissociate the aggregates.

hydration force is short range, unlike the electrostatic force, so the total potential can display one secondary potential minimum [38]. The hydration force on EYPC is high enough due to the heterogeneous composition of saturated and unsaturated lipids, which develop the existence of long-wavelength undulations of bilayers, local fluctuations in the bilayer thickness, and an increase in the motion of the hydrated head group [38,39]. Theoretical calculations [39,40] have shown that the secondary minimum is located approximately 1–2 nm away from the liposomes surface. Ions located between two liposomes are rather easily removed by dilution with water. On the other hand, DPPC or DMPC liposomes aggregate at the primary potential minimum on the liposome's surface; hence, dilution with water has no effect on the dissociation of the aggregates.

As seen in Figs. 3 and 11, there is another unusual behav-

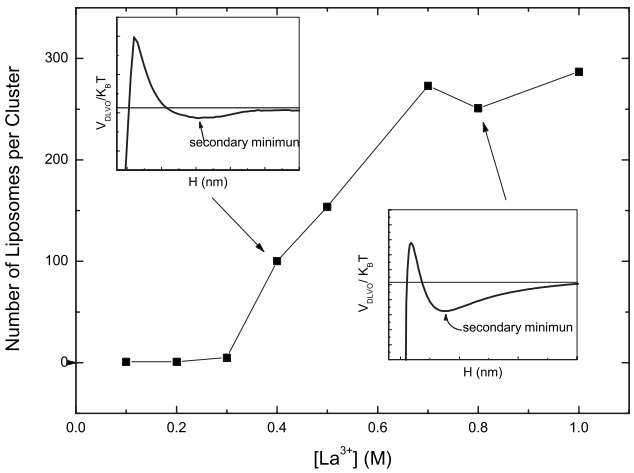

FIG. 11. Variation of the number of liposomes aggregated with the concentration of La^{3+} ions. The insets represent the secondary minimum of the DLVO potential at high and intermediate concentrations.

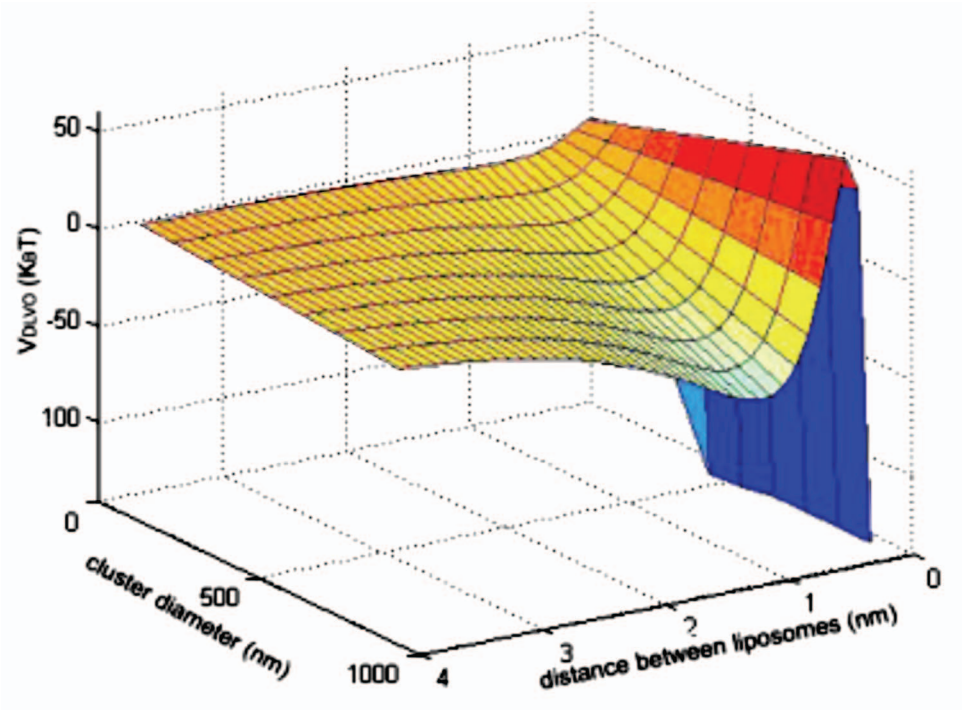

FIG. 12. (Color) DLVO potential simulation as a function of the distance between liposomes and the cluster diameter.

ior in the aggregation process of the EYPC liposomes. Usually, unstable liposomes aggregate in an infinite cluster in finite time (Fig. 3). However, in the lanthanum concentration range of 0.3 M to 0.7 M, the creation of "stationary" clusters of well-defined sizes were observed. These clusters remain stable over time.

The number of liposomes aggregated in the clusters can be calculated for each La^{3+} concentration using the equation [21]

$$n = \left(\frac{R_G}{r_o}\right)^{d_f}.$$

Results are plotted in Fig. 11.

According to the DLVO theory, the depth of the secondary minimum of the potential increases at higher salt concentrations. At intermediate concentrations (0.3 M–0.6 M), the depth of the minimum is small enough to disappear when the cluster reaches a critical number of liposomes. Figure 12 also shows that the depth of the secondary minimum does not decrease with the diameter of the cluster, therefore, we conclude that some additional factor, such as fluctuation of surface geometry or steric forces, which are not considered in the DLVO theory, should be taken into account to describe the existence of "stationary" clusters of EYPC liposomes [41,42].

IV. CONCLUSIONS

In this research, the fractal dimension of the liposome aggregations of three different types of systems, EYPC, DPPC, and DMPC, in the presence of La^{3+} have been determined. For this determination, two methods have been used, aggregation kinetics and light scattering. Variations of ζ potential associated with La^{3+} concentrations were similar for EYPC and DPPC, with a positive value which increases to 20–40 mV. However, DMPC has an initial negative value which decreases (in absolute value) to zero. In this case, the interaction between liposomes is governed only by the attractive van der Waals forces. Evolution of the aggregate sizes, followed by light scattering, shows typical behavior for DPPC and DMPC. In the case of EYPC, the final sizes of the aggregates seem to depend on the La^{3+} concentration, which permits the control of the size of stable aggregates of EYPC liposomes. The obtained fractal dimensions of the aggregates fluctuate within the range of 1.8 to 2.1.

EYPC liposomes demonstrate unusual behavior in the aggregation process: (1) The clusters return to initial size when water is added, if the final concentration of La^{3+} does not completely screen the liposome charges, (2) the hydration force on EYPC is enough to display a secondary potential minimum, and (3) the EYPC clusters are stable over time.

ACKNOWLEDGMENTS

The authors acknowledge the financial support from Spanish Ministerio de Educación y Ciencia, Plan Nacional de Investigación (I+D+i), Grant No. MAT2005-02421, from "European Regional Development Fund, (ERDF)" and by Xunta de Galicia, Grant No. PGIDIT06PXIC206048PN. P.M. thanks Fundación Antorchas, Argentina (Project No. 4308-110) for her grant.

[1] M. T. Roy, M. Gallardo, and J. Estelrich, J. Colloid Interface Sci. **206**, 512 (1998).
[2] D. D. Lasic, *Liposomes. From Physics to Applications* (Elsevier, Amsterdam, 1993).
[3] J. Pencer, G. F. White, and F. R. Hallet, Biophys. J. **81**, 2716 (2001).
[4] J. L. Burns, Y. Yan, G. J. Jameson, and S. Biggs, Langmuir **13**, 6413 (1997).
[5] S. Tang, Colloids Surf., A **157**, 185 (1999).
[6] S. R. Forrest and T. A. Witten, Jr, J. Phys. A **12**, L109 (1979).
[7] D. W. Schaefer, J. E. Martin, P. Wiltzius, and D. S. Cannell, Phys. Rev. Lett. **52**, 2371 (1984).
[8] T. Sintes, R. Toral, and A. Chakrabarti, J. Phys. A **29**, 533 (1996).
[9] K. Onuma, N. Kanzaki, and T. Kubota, J. Phys. Chem. B **107**, 11224 (2003).
[10] J. Schüler, J. Frank, W. Saenger, and Y. Georgalis, Biophys. J. **77**, 1117 (1999).
[11] M. Panouillé, D. Durand, T. Nicolai, E. Larquet, and N. Boisset, J. Colloid Interface Sci. **287**, 85 (2005).
[12] J. Liu, W. Y. Shih, M. Sarikaya, and I. A. Aksay, Phys. Rev. A **41**, 3206 (1990).
[13] I. Katsuhiro and I. Toshiaki, J. Opt. A, Pure Appl. Opt. **2**, 505 (2000).
[14] D. Majolino, F. Mallamace, P. Migliardo, N. Micali, and C. Vasi, Phys. Rev. A **40**, 4665 (1989).
[15] T. A. Witten and L. M. Sander, Phys. Rev. Lett. **47**, 1400 (1981).
[16] P. Meakin, Phys. Scr. **46**, 295 (1992).
[17] M. Kolb, R. Botet, and R. Jullien, Phys. Rev. Lett. **51**, 1123 (1983).
[18] L. M. Sander, Z. M. Cheng, and R. Richter, Phys. Rev. B **28**, 6394 (1983).
[19] P. Meakin, Phys. Rev. Lett. **51**, 1119 (1983).
[20] P. Meakin, Phys. Rev. A **27**, 1495 (1983).
[21] M. Carpineti, F. Ferri, M. Giglio, E. Paganini, and U. Perini, Phys. Rev. A **42**, 7347 (1990).
[22] A. Hasmy, M. Foret, J. Pelous, and R. Jullien, Phys. Rev. B **48**, 9345 (1993).
[23] M. Rottereau, J. C. Gimel, T. Nicolai, and D. Durand, Eur. Phys. J. E **15**, 133 (2004).
[24] M. Rottereau, J. C. Gimel, T. Nicolai, and D. Durand, Eur. Phys. J. E **15**, 141 (2004).
[25] J. Teixeira, J. Appl. Crystallogr. **21**, 781 (1988).
[26] B. Derjaguin and L. D. Landau, Acta Physicochim. URSS **14**, 633 (1941).
[27] E. J. B. Verwey and J. Th. G. Overbeek, *Theory of the Stability of Lyophobic Colloids* (Elsevier, Amsterdam, 1948).
[28] J. Sabín, G. Prieto, P. Messina, J. M. Ruso, R. Hidalgo-Alvarez, and F. Sarmiento, Langmuir **21**, 10968 (2005).
[29] J. Sabín, J. M. Ruso, A. González-Pérez, G. Prieto, and F. Sarmiento, Colloids Surf., B **47**, 64 (2006).
[30] J. Sabín, G. Prieto, S. Sennato, J. M. Ruso, R. Angelini, F. Bordi, and F. Sarmiento, Phys. Rev. E **74**, 031913 (2006).
[31] J. R. Hunter, *Zeta Potential in Colloid Science* (Academic Press, London, 1981).
[32] P. Meakin, Phys. Rev. A **29**, 997 (1984).
[33] P. Meakin, Phys. Rev. B **29**, 3722 (1984).
[34] N. J. Lynch, P. K. Kilpatrick, and G. R. Carbonell, Biotechnol. Bioeng. **50**, 151 (1996).
[35] B. Yang, K. Furusawa, and H. Matsumura, Langmuir **19**, 9023 (2003).
[36] A. S. Muresan, H. Diamant, and K. Y. C. Lee, J. Am. Chem. Soc. **123**, 6951 (2001).
[37] S. Nir, J. Bentz, and N. Düzgünes, J. Colloid Interface Sci. **84**, 266 (1981).
[38] J. Marra and J. Israelachvili, Biochemistry **24**, 4608 (1985).
[39] T. Inoue, H. Minami, and R. Shimozawa, J. Colloid Interface Sci. **152**, 493 (1992).
[40] H. Matsumura, K. Watanabe, and K. Furusawa, Colloids Surf., A **98**, 175 (1995).
[41] F. Bordi and C. Cametti, Colloids Surf., B **26**, 341 (2002).
[42] L. Stamatatos, R. Leventis, M. J. Zuckermann, and J. R. Silvius, Biochemistry **27**, 3917 (1988).